JOURNAL OF PHYSICAL ORGANIC CHEMISTRY
J. Phys. Org. Chem. 2001; **14:** 63–73

Neutral Ni(II) and Cu(II) complexes of tetraazatetraenemacrocyles

Wojciech Grochala,[1] Anna Jagielska,[1] Krzysztof Woźniak,[1] Agnieszka Więckowska,[1] Renata Bilewicz,[1] Bohdan Korybut-Daszkiewicz,[2] Jolanta Bukowska[1] and Lucjan Piela[1]*

[1]Department of Chemistry, Warsaw University, ul. Pasteura 1, 02 093 Warsaw, Poland
[2]Institute of Organic Chemistry, Polish Academy of Sciences, ul. Kasprzaka 44/52, 01-224 Warsaw, Poland

Received 25 June 2000; accepted 26 July 2000

epoc ABSTRACT: A series of electron donors [neutral Ni(II) and Cu(II) complexes of tetraazatetraenemacrocyclic ligands] differing in metal ion, size of the macrocyclic ligand, and the length of the aliphatic bridges linking the macrocyclic units in dimeric species were synthesized and their redox, structural and spectroscopic properties were studied. The x-ray results for the donors under study show a nearly planar geometry of the monomeric tetraazamacrocyclic complexes and interesting 'organic-zeolite-like' structures of the dimers. The dimeric Ni complexes have flexible cavities between the two single ligands linked with aliphatic chains suitable for accommodating some small-sized guests. For the dimeric compounds the metal oxidation [M(II)/M(III)] takes place independently on each centre except one binuclear Ni complex, where the cooperativity of the metal centres was observed. Methyl substituents give rise to irreversibility of the oxidation process of the complexes studied. In the absence of these substituents neither reorganization nor ligand addition/elimination kinetics affect the electrode process. A common scale for the donors under study and some important acceptor compounds (*p*-benzoquinone, chloranil, tetracyanoethylene and tetracyanoquinodimethane, etc.) was proposed on the basis of their cyclic voltammetric behaviour in the same physicochemical conditions. Copyright © 2000 John Wiley & Sons, Ltd.
Additional material for this paper is available from the epoc website at http://www.wiley.com/epoc

KEYWORDS: Ni complexes; Cu complexes; cyclic voltammetry; donor–acceptor systems; macrocyclic complexes; bismacrocyclic ligands; redox properties; x-ray structure; cooperative effects

INTRODUCTION

Metal ion complexes are well recognized as tunable materials owing to the dependence of their redox potential on the electronic/structural properties of ligands. The macrocyclic ligands also offer a versatile molecular scaffolding for the coordinated ions. The scaffolding provides its own structural rigidity/flexibility and may also protect (expose) the structure from (to) the environment. We describe here the synthesis and properties of a number of tetraazatetraenate Ni(II) and Cu(II) metal complexes (Fig. 1). These are either compounds synthesized for the first time (Fig. 1, M*m*, where M stands for the metal ion and $m = 14$, 15, 16 denotes the number of atoms in the macrocyclic ring of the ligand) or described elsewhere [Fig. 1, $(MmMe_2\text{-}n)_2$, $m = 15$, 16, $n = 4$, 6).[1]

Compared with the compounds reported earlier by Jäger,[2] Alcock *et al.*[3] and Busch and co-workers,[4,5] the monomeric donors studied in this work contain formyl instead of acetyl groups. Also, the monomers without methyl substituents were synthesized (Fig. 1, R = H). The compounds prepared constitute a logical series of species differing by one, two or three selected structural factors. These factors are the coordinated ion ($M = Ni^{2+}$ or Cu^{2+}), the size of the macrocyclic monomeric ligand (14-, 15- and 16-membered macrocycles), dimerization of two macrocyclic ligands (a comparison of monomers and dimers) and the length of the links connecting two monomeric moieties.

Our ultimate goal (beyond the scope of this paper) is to use the macrocyclic donors as substrates for larger dimeric/oligomeric units possessing some tailored cavities. Such a supramolecular structure may be held together by covalent, ionic or weak molecular interactions. We are interested not only in the monomeric donors but also in the dimeric ones, the latter with a variable number of the CH_2 groups linking both macrocycles. The bridge length changes the cavity size, which is crucial for the future donor–acceptor interaction. Similar donors, lacunar complexes of Co(II) and Fe(II), have been used extensively as dioxygen carriers.[5] When cavities and acceptors have appropriate size, hydrophobic/hydrophilic properties and charge distributions, then one may hope that each acceptor molecule would be

**Correspondence to:* L. Piela, Department of Chemistry, Warsaw University, ul. Pasteura 1, 02 093 Warsaw, Poland.
E-mail: piela@chem.uw.edu.pl
Contract/grant sponsor: Polish Scientific Committee; *Contract/grant number:* KBN 3 T09A 098 14.

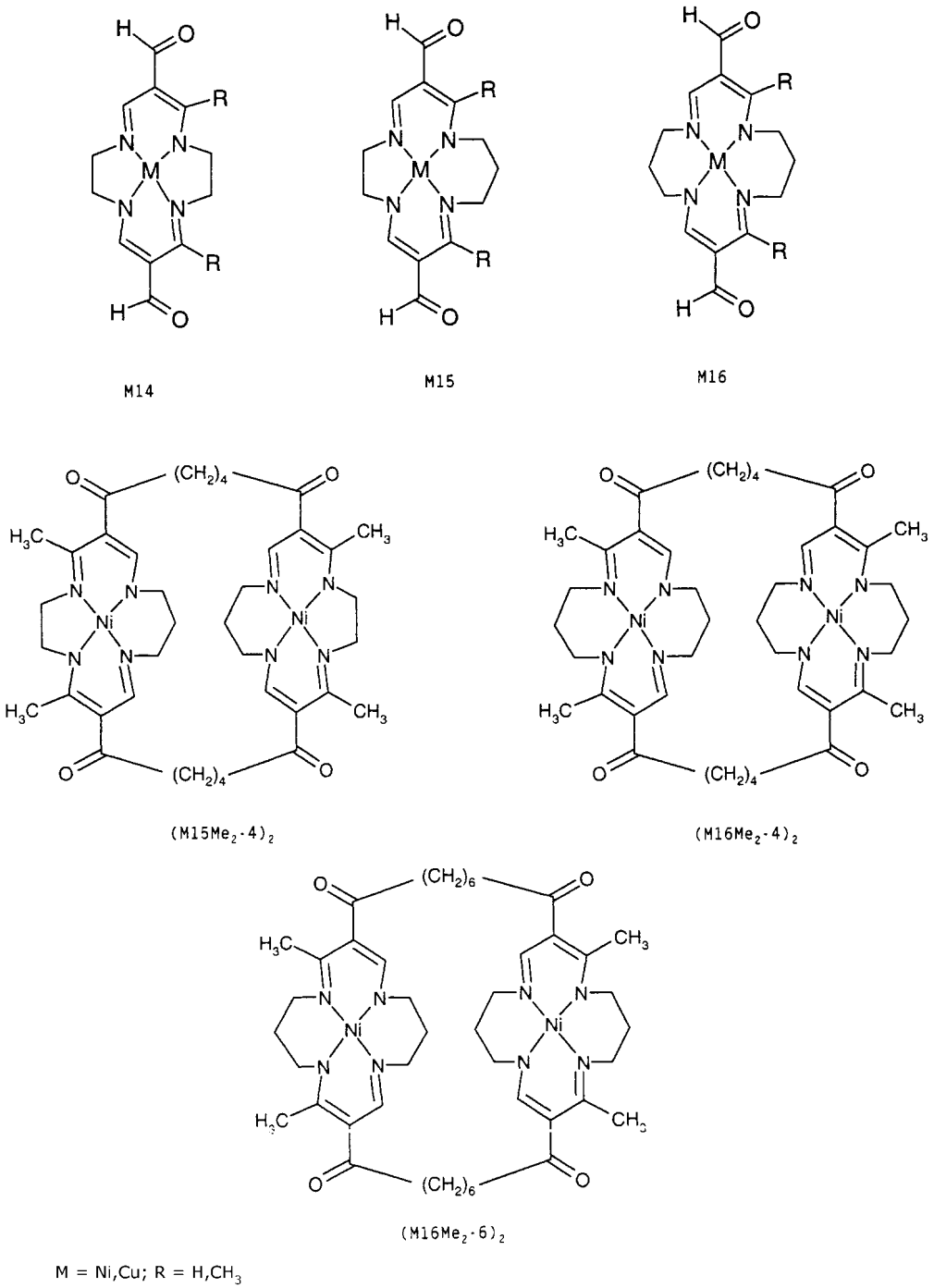

Figure 1. Tetraazaenemacrocycle ligands of Ni(II) and Cu(II) metal ions. Each macrocyclic ligand carries a formal −2e electric charge compensating that of the cation. The symbol M*m* with M = Cu, Ni and *m* = 14, 15, 16 means the corresponding metal cation (M^{2+}) and the *m*-membered macrocycle complex with R = H (for R = CH_3 the symbol M*m*Me is used). The abbreviations **(Ni16Me$_2$-4)$_2$** and **(Ni16Me$_2$-6)$_2$** represent the bismacrocyclic molecular dimers of **Ni16Me** bound by two four- and six-membered methyl units, respectively

docked between a pair of donors. This may result in a number of novel applications of such complex donor (D)–acceptor (A) systems, e.g. allowing charge transfer in several adjacent DA units or even generating electronic bistability.[6,7]

The purpose of this study was to select the most promising DA pairs for such study applications, i.e. pairs with the smallest difference of the redox potentials. Therefore, *p*-benzoquinone (Q), chloranil (CA), tetracyanoethylene (TCNE) and tetracyanoquinodimethane (TCNQ) were proposed as acceptors and placed on a common redox potential scale. The abbreviations given in Fig. 1 will be used throughout this paper.

In addition to structural properties solute–solvent

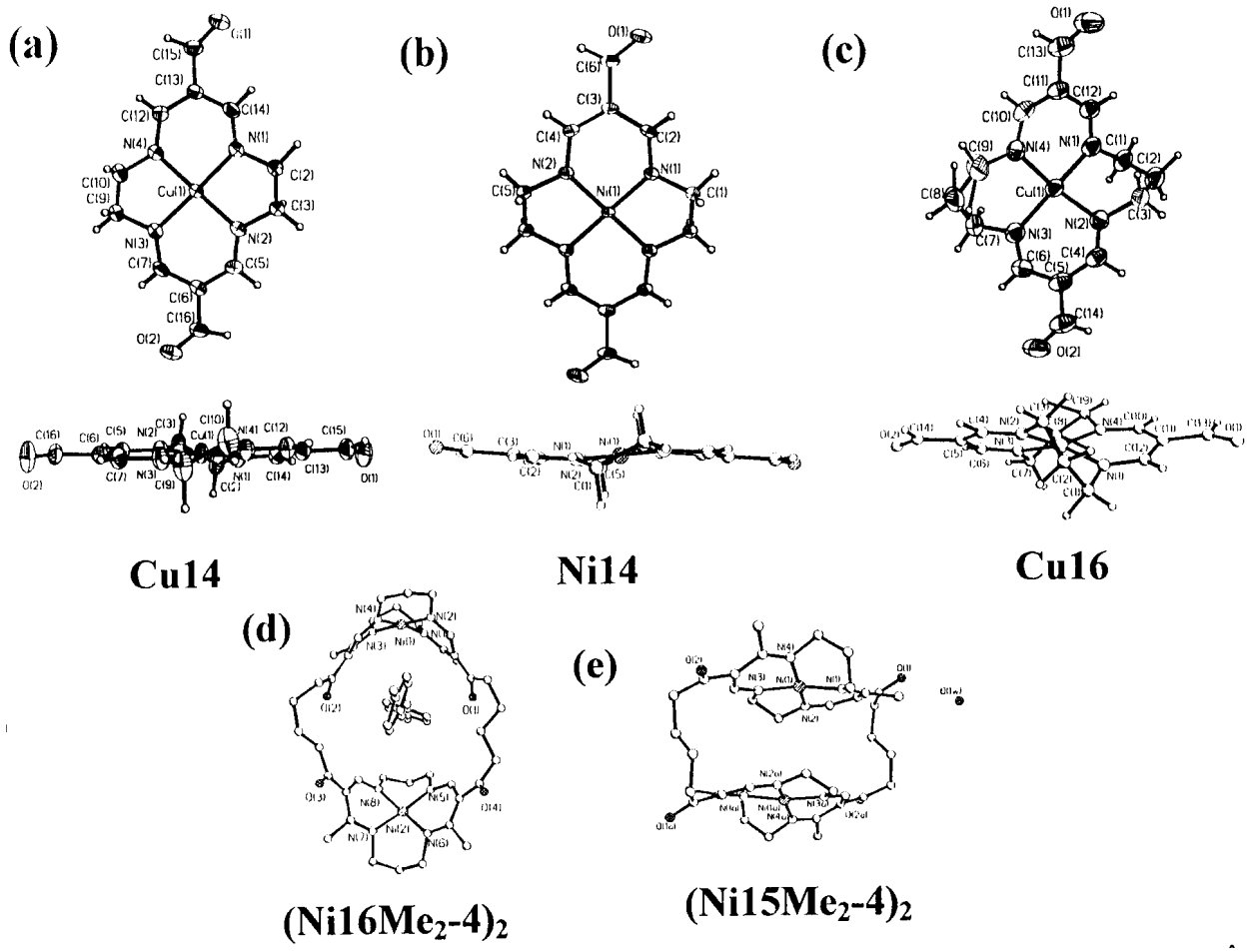

Figure 2. Molecular structure of monomeric donors obtained from the crystallographic measurements: (a) **Cu14**; (b) **Ni14**; (c) **Cu16**. All monomeric compounds are almost square planar (see Table 1). Molecular structures of dimeric donors (Ref. 1) are shown in (d) **$(Ni16Me_2\text{-}4)_2$** and (e) **$(Ni15Me_2\text{-}4)_2$**. In contrast to **$(Ni15Me_2\text{-}4)_2$**, the **$(Ni16Me_2\text{-}4)_2$** structure hosts disordered toluene molecules in the cavities between strongly deformed macrocyclic fragments linked with two aliphatic chains. Only non-hydrogen atoms are shown for the bismacrocycles

interactions are known as important factors in redox processes.[8,9] Hence tuning of the redox potential differences is meaningful only when done in the same solvent, for both donors and acceptors. With this in mind we chose acetonitrile (AN), a solvent suitable for both polar and non-polar compounds and convenient for electrochemical studies owing to its high dielectric constant (∼36).

EXPERIMENTAL AND COMPUTATIONAL PROCEDURE

Details of syntheses, *ab initio* calculations, x-ray diffraction crystallographic studies, Raman spectroscopy, UV–VIS, NMR, mass spectrometric and voltammetric measurements are given in the Supplementary Material.

Crystallographic data (excluding structural factors) for the structures reported in this paper have been deposited with the Cambridge Crystallographic Data Centre and allocated the deposition numbers CCDC 121699, CCDC 121700 and CCDC 121701 for **Cu14, Cu16** and **Ni14**, respectively. Copies of the data can be obtained free of charge on application to CCDC (E-mail: deposit@ccdc.cam.ac.uk).

RESULTS AND DISCUSSION

Geometric features

The monomeric ligands studied in this work are neutral species composed of two strongly delocalized 7π-electron systems separated by aliphatic links and coupled by the bridging metal ion. This situation is often formally depicted as each of the two systems carrying −1e electric charge compensated by the +2e charge at the coordinated cation. Structural features of the ligands were studied in the solid state by x-ray crystallography and for the isolated molecules by *ab initio* calculations. According to

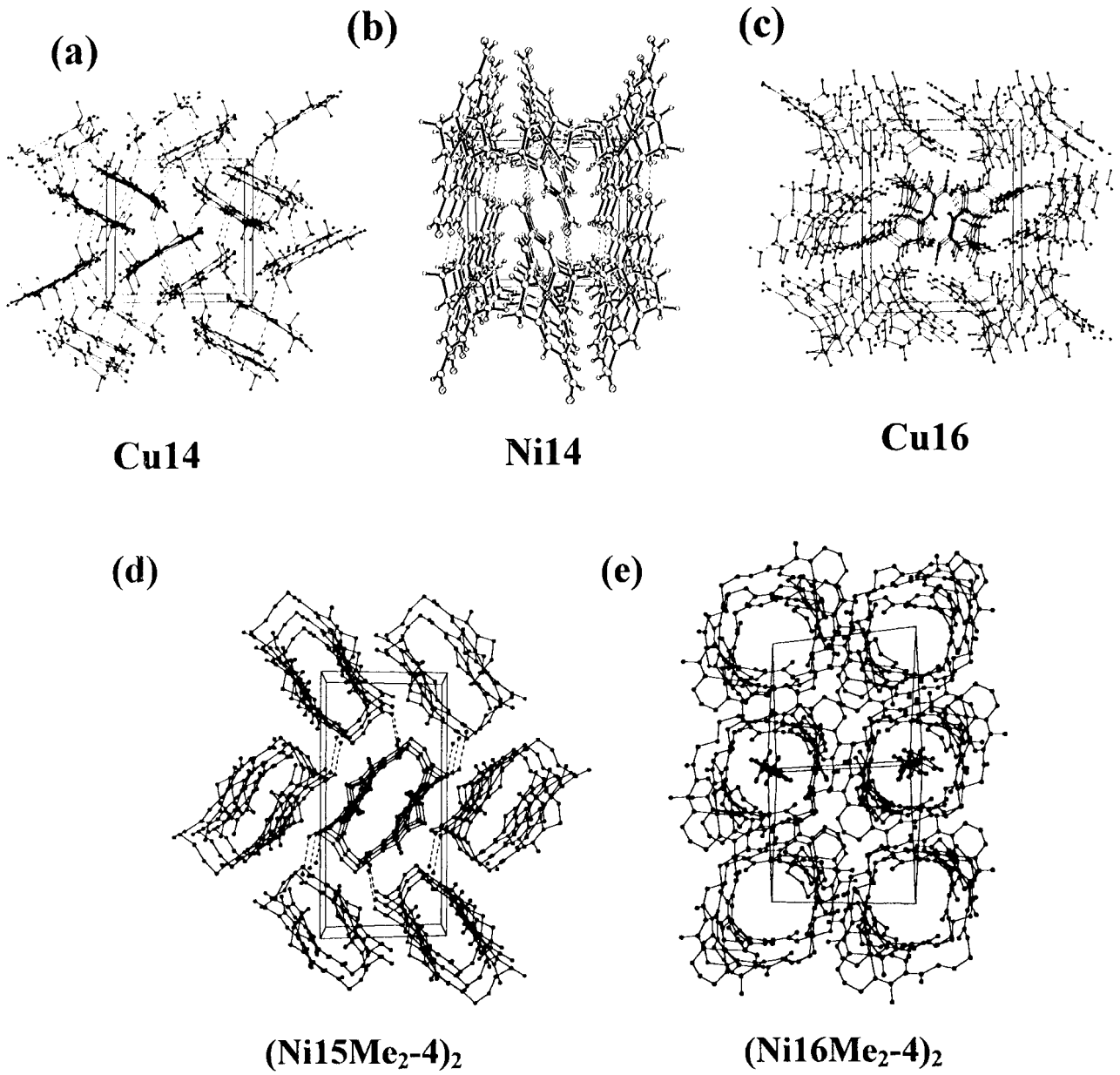

Figure 3. Illustration of the crystal packing and short contacts such as C—H···O and Me···O interactions (dotted lines) in (a) **Cu14**, (b) **Ni14** and (c) **Cu16**. Zeolite-like structure of the bismacrocycles: (d) **(Ni15Me$_2$-4)$_2$** with water molecules between the stacked column of the bismacrocycle and (e) **(Ni16Me$_2$-4)$_2$** with disordered toluene molecules in the cavities of the bismacrocycles[1]

our calculations (Restricted Open-Shell Hartree–Fock level, 6–31G* basis set[10]) the charge distribution for the isolated moieties resembles only qualitatively the above picture. The Mulliken net charge on the metal atom is +1.48e and +1.62e instead of +2e, and on the NC_3N fragments one has −1.14e and −1.20e instead of the formal −le charge for the **Ni14** and **Cu14**, respectively. The calculations show that all the bonds are strongly polar with the largest polarization being at the complex centre, and the most negative net charges are carried by the four nitrogen atoms.

According to the x-ray results, the molecular structures of the monomeric **Cu14**, **Ni14** and **Cu16** complexes exhibit different degrees of planarity. **Ni14** and **Cu14** are almost square planar (Figs 2 and 3, Table 1), whereas **Cu16** is significantly distorted from planarity. Some small differences among the Ni—N distances, and also among the Cu—N distances, are within the level of errors. From the crystallographic point of view, only the **Ni14** molecule is a symmetric molecule in the crystal lattice with the nickel atom at the symmetry centre (C_i symmetry group). The *ab initio* Hartree–Fock (6–31G basis set) geometry optimization gives also C_i symmetry for the isolated **Ni14** molecule (for **Cu14** the calculations

Table 1. Geometry of the central NiN_4 fragment: deviation from square-planar symmetry[a]

Compound	Deviation of metal ion	Deviations of the nitrogen atoms	Metal—N bond lengths	Deviations of the aromatic carbon atoms
Ni14	0.000	0.00, 0.00, 0.00, 0.00	1.858, 1.856, 1.858, 1.856	0.31, −0.28, 0.28, −0.31
Cu14	0.025	0.13, −0.13, 0.13, −0.13	1.933, 1.927, 1.935, 1.921	0.35, −0.35, 0.36, −0.36
Cu16	0.030	0.47, −0.45, 0.42, −0.45	2.081, 1.993, 2.150, 1.957	1.13, 0.15, −0.97, 0.44, −0.05, −0.92
(Ni15Me$_2$-4)$_2$	0.008	0.13, −0.15, 0.15, −0.14	1.881, 1.845, 1.891, 1.817	−0.60, −1.41, −0.81, −0.77, −1.64, −0.85, 0.91, 1.72, 0.86, 0.56, 1.49, 0.63
(Ni15Me$_2$-4)$_2$	−0.077, −0.066	0.06, −0.06, −0.05, 0.06 0.02, −0.02, 0.02, −0.02	1.897, 1.874, 1.900, 1.843 1.871, 1.900, 1.895, 1.887	0.13, −0.19, −0.87, −0.04, 0.86

[a] A deviation of an atom represents the distance in Å of the corresponding atom from the best plane based on the nitrogen atoms.

give C_2 symmetry, with the symmetry axis going through the metal atom, M, and almost orthogonal to the best plane of the MN_4 system). The *ab initio* calculations for **Ni14** show that the Ni···N distances are very close to 1.92 Å and 1.87 Å at the Hartree–Fock and the density functional theory (DFT/B3LYP) levels, respectively, The consecutive N—Ni—N angles are 85.9, 94.1, 85.9 and 94.1° at the HF level and 86.2, 93.8, 86.2 and 93.8° at the DFT/B3LYP level. The M···N distances in **Cu14** are slightly longer, 1.96 and 1.93 Å at the HF and DFT/B3LYP levels, respectively. The consecutive N—M—N angles in **Cu14** are 85.7, 94.9, 85.7 and 94.9° at the HF level and 85.7, 94.7, 85.7 and 94.6° at the DFT/B3LYP level. The DFT/B3LYP results for the M···N distances agree to within 0.01 Å with the experimental values, much better than the Hartree–Fock results. The M···N bond lengthening (0.04 and 0.06 Å for HF and DFT/B3LYP, respectively) is consistent and larger than the difference of the Shannon's ion radii (0.02 Å[11]) The *ab initio* Hartree–Fock geometry optimization for the isolated molecules (starting from the x-ray configuration) gives also the planar fragments, with a very small $OC_{CHO}C_{ar}C_{ar}$ dihedral angle, of the order of 0.4° for **Cu14** and 2.3° for **Ni14**, and the C_{ar}—C_{CHO} bond lengths typical for aromatic systems, about 1.43 Å.

The central MN_4 fragment exhibits a higher symmetry (close to C_{2h}) than that of the whole molecule. Since the deviation of the central MN_4 fragment from the square planar symmetry is fairly small for both **Cu14** and **Ni14**, one may anticipate that the spectroscopic alternative rule will be approximately obeyed for some bands. The calculations give information about π-conjugation effects for **Ni14** and **Cu14**. The C—C bonds in the π-electron region are almost equal to the characteristic bond length of 1.42 Å. The C—N bond lengths are close to about 1.30 Å for all the C_{ar}—N bonds and to 1.42–1.46 Å for all the C_{aliph}—N bonds. The equality of the C_{ar}—N bond lengths suggests that the π-conjugation is extended over the region between the two nitrogen atoms, although the bond length is only slightly larger than that typical for the CN double bond (1.28 Å). In agreement with this, the C_{aliph}—N bond length is close to a typical single C—N bond length (1.47 Å). The formyl groups in **Ni14, Cu14** and **Cu16** participate in the π-conjugated system. The x-ray diffraction data confirm their near-coplanarity with the central π-electron part, especially for the 14-membered macrocycles. Indeed, the angles between each of the two formyl group planes and the best four-nitrogen plane are both equal to 9° for **Ni14** (centre of symmetry), 14 and 6° for **Cu14** and 21 and 24° for **Cu16**. The intermolecular contacts in **Cu14** and **Ni14** crystals are different (Fig. 3). The central Cu^{2+} cation has some close contacts (about 3.335 Å) with symmetry $[1/2 + x, 1/2 - y, -z]$ related O(2) atom and about 3.19 Å with H(10a) from the neighbouring $[1 - x, -1/2 + y, 1/2 - z]$ molecule the closest in the crystal lattice. Both the oxygen atoms interact with —CH groups, O(1) with H(9b) $[1 + x, y, z]$, ca 2.48 Å, and O(2) with H(2b) $[-1 + x, y, z]$, ca 2.32 Å, and H(9a) $[x, y, -1 + z]$, ca 2.38 Å. The arrangement of **Ni14** molecules in the crystal lattice is such that some intermolecular dimers are formed via weak C—H···O interactions with the H···O distance 2.42 Å, with the H···O distance 2.42 Å, O(1)···H(1b) $[1-x, 1-y, 1-z]$. Such a weak dimer interacts with another one located more or less perpendicularly in such a manner as to facilitate the M···H close contacts of about 3.16 Å to H(1a) $[-x, 1/2 + y, 1/2 - z]$ (Fig. 3). In the case of **Cu14** the situation is similar with the closest M···H contact only slightly longer (3.19 Å). However, in contrast to **Cu14**, there is no close M···O contacts.

The **Cu16** molecules also form molecular dimers in the crystal (Fig. 3), interacting with the neighbouring moieties *via* weak C—H···O hydrogen bonds (ca 2.4 Å). These H-bonds are only slightly longer than those in the **Ni14** and **Cu14** cases, 2.58 and 2.87 Å from O(1) to

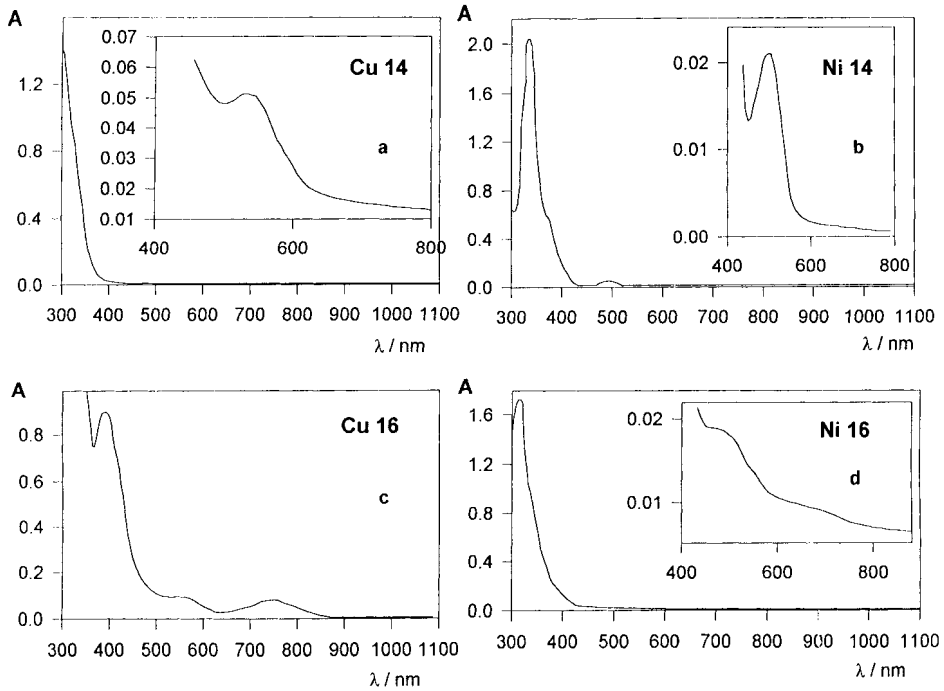

Figure 4. Electronic absorption spectra (*A* means absorbance) of saturated donor solutions in a 1:1:1 mixture of CH_3CN, CH_3OH, CH_3Cl: (a) **Cu14**; (b) **Ni14**; (c) **Cu16**; (d) **Ni16**

H(7a) $[-x, -y, 2 -z]$ and H(2a) $[-1 - x, -y, 2 - z]$, respectively. The shortest intermolecular H···O contacts for the O(2) atom are even longer and equal to ca 2.9 Å. Also, the shortest M···O (4.33 Å) and M···H (3.68 Å) contacts for **Cu16** are ca 1 Å longer than for the other monomers.

Spectroscopic results

Figure 4 shows a section of the electronic absorption spectra and Table 2 presents the wavelengths of several electronic transitions observed in the UV–VIS spectra of the donors in the solution. In the analysis of electronic transitions one has to take into account the d–d, LMCT, MLCT, π–π* and n–π* transitions.

Most of the donors studied have three evident absorption bands in the 300–1100 nm range (the 800–1100 nm region was blank and hence is not shown in Fig. 4). There is a very strong single band at 300–390 nm and a shoulder at about 330–370 nm. This strong single band may be assigned to the ligand-centred π–π* transitions in analogy with the Soret band[12] with a large molar absorption coefficient ($\varepsilon \approx 5 \times 10^3$ l mol^{-1} cm^{-1}). There is no clear tendency of energy decrease of the strong UV band as the structure becomes flatter (Table 2). The strong band at about 320 nm is almost insensitive to the ligand ring distortions [compare the λ values for **Ni16Me$_2$** and **(Ni16Me$_2$-4)$_2$**] and to the ring substituted with methyl groups (compare the λ values for **Ni16Me$_2$** and for **Ni16**). This suggests that the band at about 300 nm originates from a local N,C-centred π–π* transition.

The lowest-energy transition of small intensity is observed for all compounds at about 480–550 nm. This seems to be due to the π–π* electronic transition (HOMO–LUMO, an analogue of a Q porphyrin band[12]) with a strong contribution from the carbonyl groups (thus having a partial n–π* character also).

The IR, Raman and RR spectra all of the donors

Table 2. Wavelengths, λ (nm), and the assignment of the electronic transitions for the donors under study

Transition	**Cu14**	**Cu16**	**Ni14**	**Ni15**	**Ni16**	**Ni16Me$_2$**	**(Ni16Me$_2$-4)$_2$**	**Ni16Me$_2$-6)$_2$**
(π–π*)	300 vs	ca.300	335 vs	329 s	320 vs	321 vs	320 vs	315 vs
(π–π*)	330 sh	390 vs-	370 sh	375 sh	370 sh	425 sh	–	–
(π–π*) + (n–π*)	530 w	550 w	490 w	512 w	490 w	480 w	480 m	490 w
LMCT		750 w			650vw			

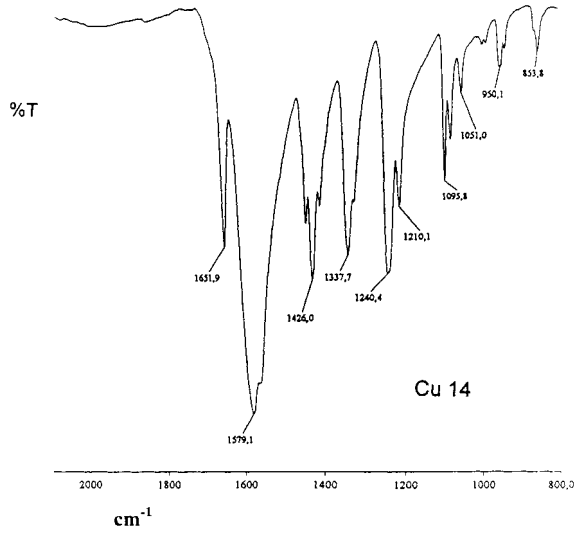

Figure 5. IR spectrum of **Cu14**

studied here are similar and related to those of the analogous metalloporphyrins.[12] This is the reason why we present only a representative example of the IR, Raman and RR spectra (Figs 5 and 6). The full set of the IR, Raman and RR spectra are included in the **Supplementary Material**.

An approximate square-planar symmetry of the central part of the **Ni14** and **Cu14** molecules may explain qualitatively the relative intensities of the Raman and IR spectra. The vibrations localised mainly in the centre should approximately exhibit C_{2h} symmetry. As a consequence, most of the IR-active modes are Raman inactive and vice versa, which is confirmed by the calculated IR intensities. If the symmetry of **Cu14** and **Ni14** were indeed C_{2h}, their molecular vibrations might be decomposed as Γ = Raman (31 A_g + 14 B_g) + IR (32 B_u + 16 A_u). The same small deviations from the C_{2h} symmetry explain why in reality the A_g modes have negligible IR intensities (typically 0.0–0.2 km mol^{-1}), and the B_g modes are also practically forbidden in the IR spectra (0.0–2.9 km mol^{-1}).[13] If the molecular symmetry were D_{2h}, which is still close to reality for the central part of the complexes, the A_u modes would be forbidden in the IR. This seems to be the reason why in the IR the A_u modes are much weaker (usually 4.8–22.1 km mol^{-1}) than the B_u modes (typically strong or very strong, up to 239 km mol^{-1}). Of course, the assignment based on C_{2h} symmetry fails for the modes containing strong contribution from the alkyl bridges (element decreasing molecular symmetry).

Electrochemical results

Stronger donor abilities are manifested voltammetrically by a decrease in the formal potential of the Ni(II)–Ni(III) or Cu(II)–Cu(III) systems (Fig. 7 and Table 3). A promising donor would exchange electron reversibly and no chemical reactions should interfere with this process.

Almost reversible electrode behaviour for **Ni14**, **Ni16** and **Cu14** was demonstrated by the close to unity ratio of the cathodic to anodic peak currents and the peak potential differences, $E_{pa} - E_{pc}$, close to 60 mV. The oxidation of **Cu14** proceeds at less positive potentials than that of **Ni14**, indicating better electron donor properties of the former. For the 14-membered monomeric ligands, **Cu14** oxidizes more easily than **Ni14**, whereas the opposite occurs for **Cu16** and **Ni16**. Hence the formal potential of the M(II)–M(III) complex couple is determined by both the electronic and structural factors. The reversibility of the **Cu14** system suggests that both the Cu(II) and Cu(III) forms appear in a similar planar configuration, so the electron release does not require larger reorganization of the complex. The planarity, the high redox reversibility and a low value of the formal potential for **Cu14** make it one of the most promising of the electron donors under study.

Changes of substituents or of the macrocyclic ligand size affect both the potential at which the complex is oxidized (Fig. 7) and the reversibility of the system. A lower reversibility of the non-planar **Cu16** vs the planar **Cu14** and **Ni14** vs **Ni16** indicates larger structural changes accompanying the electron transfer in those cases. Also, the substitution of **Ni16** with two additional methyl groups (Jäger-type complexes[2]) introduces chemical irreversibility.

Influence of dimerization and the double bridge length

Figure 2 shows the molecular structure of the **(Ni15Me$_2$-4)$_2$** and **(Ni16Me$_2$-4)$_2$** complexes.[1] Both Ni(II) dimers have large cavities formed between the macrocycle moieties joined by two aliphatic chains. The bismacrocyclic Ni(II) receptors form unique 3D structures containing parallel channels (Fig. 3)—an 'organic zeolite.' The channels can be occupied by some smaller guest molecules (e.g. H_2O, $CHCl_3$ or toluene). According to x-ray results, there is an umbrella-like distortion of the monomers of the dimeric ligands especially for **(Ni16Me$_2$-4)$_2$**, owing to the tension in the too short aliphatic links. These structural changes may result in more facile oxidation of the metal ion in the dimeric species with respect to the monomer (Table 3 and Fig. 7). The anodic peak for the two bismacrocycles is twice as high as those for the single macrocycle compounds since two redox centres are present in one molecule of the bismacrocyclic complexes. However, lack of the cathodic counterparts of these peaks reveals following chemical reactions of the Ni(III) oxidation product.

The appearance of two oxidation signals may be

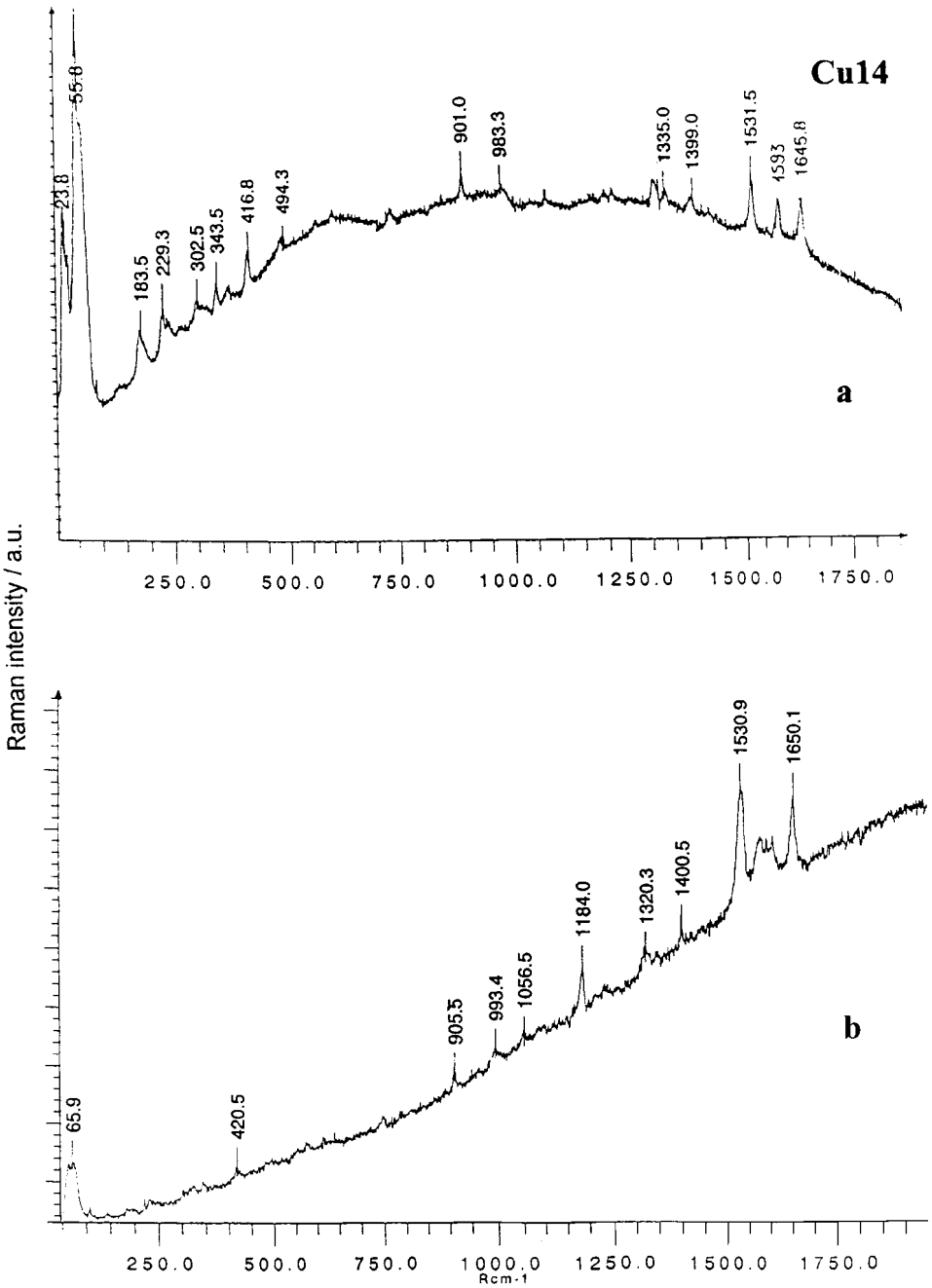

Figure 6. Raman spectra of **Cu14** excited with (a) 647.1 and (b) 488 nm radiation

expected for two identical redox centres when in close proximity. In the case of the **(Ni16Me$_2$-4)$_2$** and **(Ni16Me$_2$-6)$_2$** complexes, the appearance of a single, but twice as high, oxidation peak means that both centres are separated well enough and do not interact, so voltammetrically they behave as two independent Ni(II) sites. Our x-ray analysis gives for the intermetallic distance 9.3 Å for **(Ni16Me$_2$-4)$_2$**. Thus, assuming small crystal packing effects, the electrostatic interaction in acetonitrile (AN) seems to be effectively shielded at such distances. In contrast, for **(Ni15Me$_2$-4)$_2$** a much shorter intermetallic distance is found from the x-ray measurements (5.22 Å). Therefore, a splitting of the oxidation peak in AN solution is observed (see Table 3 and Fig. 7) which reflects the cooperativity of the metal centres.

The electronic spectrum of **(Ni16Me$_2$-4)$_2$** does not show large differences in comparison with **Ni16**. Therefore, not only the positively charged metal centres are effectively shielded by the solvent as demonstrated by electrochemistry, but also the interaction of the π-electron systems of the two macrocycles is fairly small.

The dimerization influences more strongly the vibra-

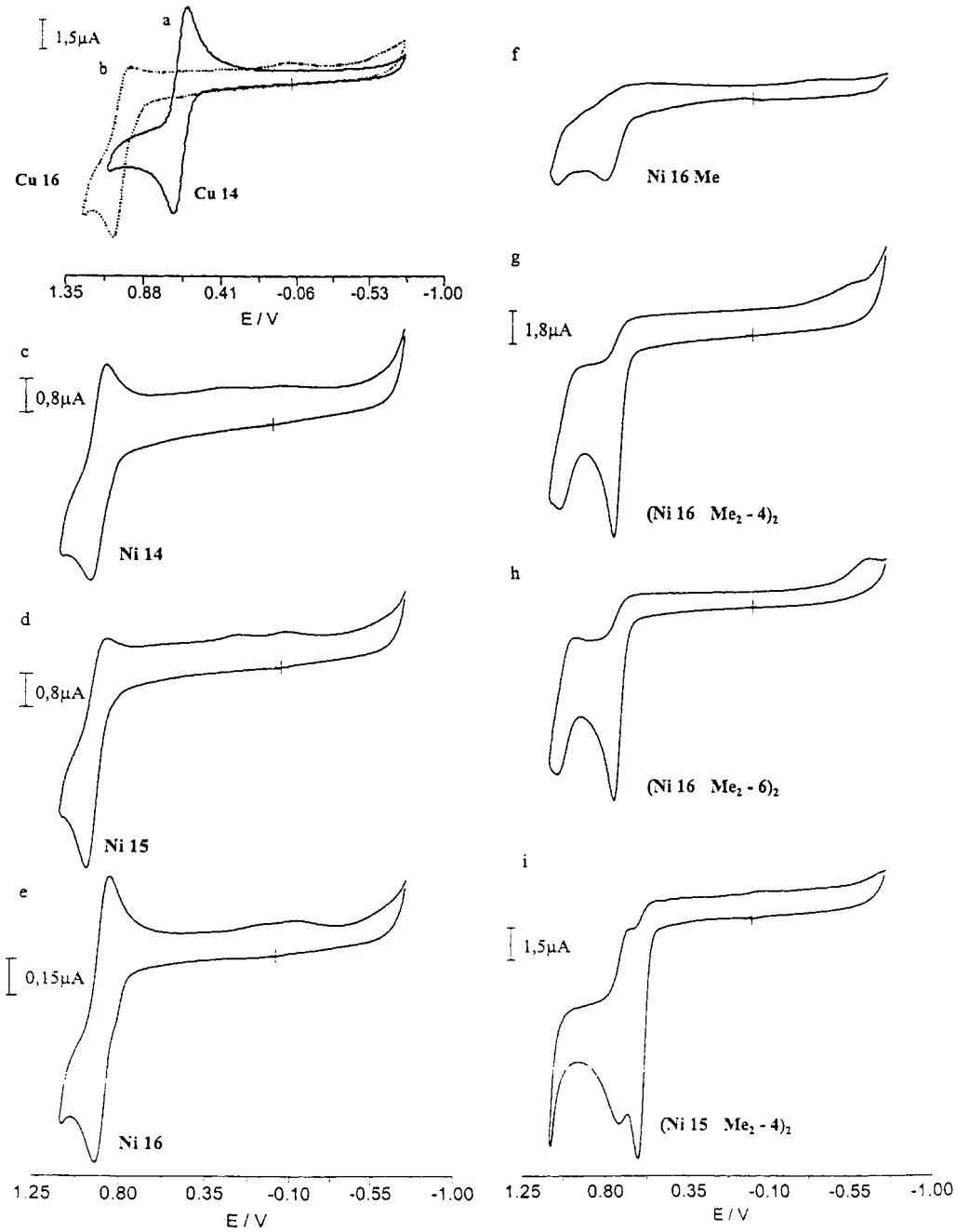

Figure 7. Redox properties of the tetraazaenemacrocyclic complexes of Cu^{2+} and Ni^{2+}. CV curves for 0.4 mM **Cu14** (a), **Cu16** (b), **Ni14** (c), **Ni15** (d), **Ni16** (e), **Ni16Me** (f), **(Ni16Me$_2$-4)$_2$** (g), **(Ni16Me$_2$-6)$_2$** (h) and **(Ni15Me$_2$-4)$_2$** (i) in 0.1 M a TBAP solution of acetonitrile, scan rate 0.05 V $s.^{-1}$ The figure shows the oxidation potential dependence on the metal ion [(a) vs (c), (b) vs (e)], of the macrocycle size [(a) vs (b), (c) vs (d) and (e), (g) vs (i)] of the methyl substitution [(e) vs (f)], of the dimerization [(f) vs (g), (e) vs (g), (f) vs (h), (e) vs (h), (d) vs (i)] and of the bridge length [(g) vs (h)]. (a), (c) and (e) show the reversible oxidation processes. Note the cooperativity of oxidation in case (i)

tional spectra of the complexes than does the length of the macrocycles. The wavenumber differences among **Ni14, Ni15** and **Ni16** are usually smaller than those among the monomeric and dimeric units. As can be seen in Fig. 2, especially the umbrella-like out-of-plane deformation of the aromatic rings is an important structure determining factor of the dimers. The differences between **(Ni16Me$_2$-4)$_2$** and **(Ni16Me$_2$-6)$_2$** are less important, the compounds have also similar oxidation peak potentials (0.752 and 0.747 V, respectively) and the size of the hydrophobic cavity seems to be the only structurally relevant difference between them.

Table 3. Voltammetric characteristics of the donor compounds in AN–0.1 M TBAP solution (see Experimental section, voltammetry), scan rate 0.05 Vs^{-1}[a]

Compound	E_{pa} M(II)/M(III)	E_{pc} M(III)/M(II)	$E^{0'}$ M(II)/M(III)	$E_{pa} - E_{pc}$
Cu14	0.698	0.630	0.664	0.068
Ni14	0.947	0.867	0.907	0.080
Ni15	0.957	0.859	0.908	0.098
Cu16	1.060	0.972	1.016	0.088
Ni16	0.913	0.850	0.882	0.063
$Ni16Me_2$	0.800			
$(Ni15Me_2\text{-}4)_2$	0.615 and 0.737[b]			
$(Ni16Me_2\text{-}4)_2$	0.756			
$(Ni16Me_2\text{-}6)_2$	0.747			

[a] The formal potentials are given only for the systems with well developed anodic/cathodic peaks; blanks mean that the cathodic signal is absent owing to chemical reaction consuming the oxidized form of the complex following electron transfer as described in the text. E_{pa} and E_{pc} denote the oxidation and reduction peak potentials, respectively, and E^0 is the formal potential. All potentials are in volts.
[b] The splitting of the peaks is due to an oxidation cooperativity between the two Ni(II) centres.

Common redox scale for donors and acceptors

The goal of this work was to select those donor–acceptor pairs, which exhibit very close redox potentials when measured in the same solvent. In the AN solutions the reduction of all the acceptors under study, quinone,[14] chloranil,[15] tetracyanoquinodimethane[16] and tetracyanoethylene,[17] proceeds in two well resolved 1e redox steps with the formation of a radical and dianion, respectively. Table 4 gives the peak and formal potentials, which show the following sequence of the redox potentials: TCNE ≈ TCNQ > CA ≫ Q, in line with the *ab initio* calculated electron affinities (Hartree–Fock, 6–31G* basis set, adiabatic approximation, vacuum conditions): TCNQ ≈ CA ≈ TCNE ≫ Q [TCNQ (2.94 eV), CA (2.85 eV), TCNE (2.76 eV), Q (1.31 eV)].

The formal potentials for the acceptors and donors are shown in Fig. 8. They were all measured under the same experimental conditions [obtained from cyclic voltammetry (CV) with the use of a glassy carbon electrode in AN]. For the two donor–acceptor pairs **Cu14**–TCNQ and **Cu14**–TCNE, the electric potential differences are the smallest and are as small as 0.430 and 0.373 V, respectively. This suggests that the **Cu14**–TCNQ and **Cu14**–TCNE redox pairs can be considered as promising building blocks for bistable molecules[6,7] and new donor–acceptor materials.

CONCLUSIONS

The x-ray results for the donors studied show a nearly planar geometry of the monomeric tetraazamacrocyclic complexes and an 'organic-zeolite-like' structures of the dimers. The dimeric Ni complexes have flexible cavities between of the two single ligands linked with aliphatic chains suitable for accommodating some small-sized guests.

For the dimeric compounds the metal oxidation [M(II)–M(III)] takes place independently on each centre except for **$(Ni15\text{-}Me_2\text{-}4)_2$** where, owing to the short metal–metal distance, an oxidation cooperativity has been observed. Methyl substituents give rise to irreversibility of the oxidation process of the complexes studied. In the absence of these substituents neither reorganization nor ligand addition–elimination kinetics affect the electrode process. This suggests that the **Cu14** can be considered as a promising donor for new donor–acceptor complexes.

A common scale for the donors under study and some important acceptor compounds (*p*-benzoquinone, chloranil, tetracyanoethylene and tetracyanoquinodimethane,

Table 4. Characteristics of the cyclic voltammograms of acceptor molecules in AN–0.1 M TEAP solution scan rate: 0.05 V s^{-1}[a]

Compound	E_{pc1}	E_{pal}	$E^{0'}{}_1$	E_{pc2}	E_{pa2}	$E^{0'}{}_2$
TCNE[b]	0.237	0.344	0.291	−0.784	−0.694	−0.739
TCNQ	0.200	0.269	0.234	−0.352	−0.278	−0.315
Q	−0.520	−0.450	−0.485	−1.210	−1.130	−1.170
CA	0.044	0.117	0.0805	−0.732	−0.649	−0.690

[a] E_{pc1}, E_{pa1}, E_{pc2} and E_{pa2}, are the peak potentials for the first and second electron transfer, respectively, and $E_1^{0'}$, $E_2^{0'}$ are the formal potentials. All potentials in volts.
[b] TCNE in 0.1 M TBAP–CH_2Cl_2; scan rate 0.02 V s^{-1}.

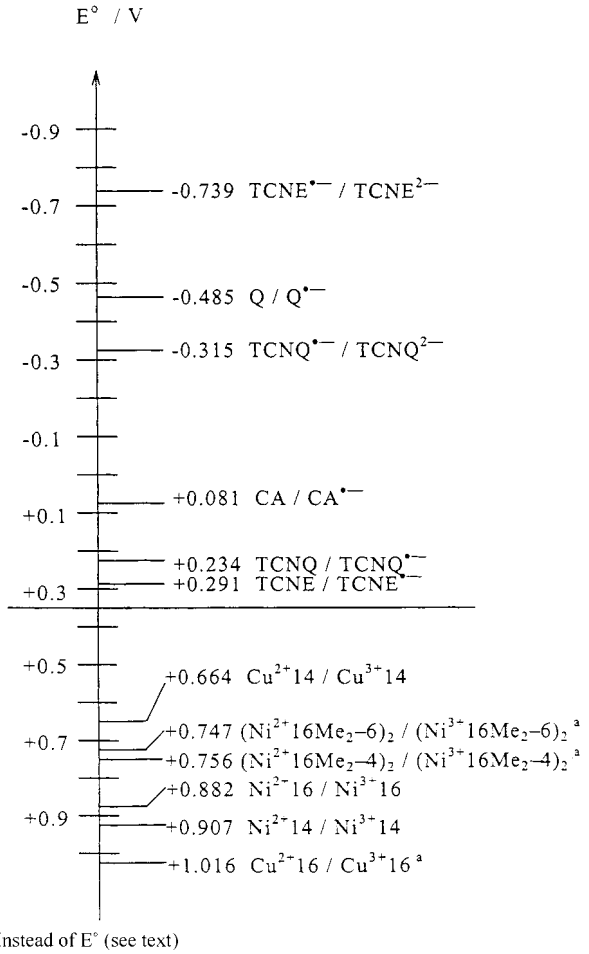

Figure 8. Positioning of the donors and acceptors under investigation in the common electric redox potential scale (*E* in volts). The potentials were measured under the same conditions: 0.1 M TBAP in AN, scan rate 0.05 V s.$^{-1}$ A promising donor–acceptor pair, candidate for the bistability effect (in AN), corresponds to a donor oxidation potential slightly lower than the acceptor reduction potential (e.g. **Cu14**–TCNE or **Cu14**–TCNQ)

etc.) was proposed on the basis of their CV behaviour under the same physicochemical conditions. This scale allowed us to select the **Cu14**–TCNQ and **Cu14**–TCNE redox pairs as good candidates for the building blocks of an electronically bistable molecule.

Acknowledgements

Provision of NIR–Raman equipment by Professor P. Wrona and the technical help of Dr P. Piela are gratefully acknowledged. This work was supported financially by the Polish Scientific Committee, project KBN 3 T09A 098 14. B.K.D. acknowledges financial support within the KBN project 3 T09A 076 15. In the computational part we benefitted from the computational resources of the Interdisciplinary Centre for Mathematical and Computational Modelling, Warsaw University.

REFERENCES

1. Bilewicz R, Więckowska A, Korybut-Daszkiewicz B, Feeder N, Woźniak K. *J. Phys. Chem.* 2000; **104**: 11430–11434.
2. Jäger EG. *Z. Chem.* 1968; **8**: 392–393.
3. Alcock NW, Lin WK, Jarcitano A, Mokren J. Do, Corfield PWR, Johnson G, Novotnak G, Cairns C, Busch DH. *Inorg. Chem.* 1987; **27**: 440–452.
4. Kolchinski AG, Korybut-Daszkiewicz B, Rybak-Akimova EV, Busch DH, Alcock NW, Clase HJ. *J. Am. Chem. Soc.* 1997; **119**: 4160–71.
5. Busch DH, Alcock NW. *Chem. Rev.* 1994; **94**: 585–623.
6. Stolarczyk LZ, Piela L. *Chem. Phys.* 1984; **85**: 451–460.
7. Nowaczek W, Piela L, Stolarczyk LZ. *Advan. Mater Opt. Electron.* 1996; **6**: 301–306.
8. Mann CK. In *Electroanalytical Chemistry*, Bard A (Ed), vol 3. Marcel Dekker: New York, 1969: 60–70.
9. Hubig SM, Rathore R, Kochi JK. *J. Am. Chem. Soc.* 1999; **121**: 617–626.
10. Frisch MJ, Trucks GW, Schlegel HB, Gill PMW, Johnson BG, Robb MA, Cheeseman JR, Keith T, Petersson GA, Montgomery JA, Raghavachari K, Al-Laham MA, Zakrzewski VG, Ortiz JV, Foresman JB, Cioslowski J, Stefanov BB, Nanayakkara A, Challacombe M, Peng CY, Ayala PY, Chen W, Wong MW, Andres JL, Replogle ES, Gomperts R, Martin RL, Fox DJ, Binkley JS, Defrees DJ, Baker J, Stewart JP, Head-Gordon M, Gonzalez C, Pople JA. Gaussian 94, Revision D.3. Gaussian: Pittsburgh, PA, 1995.
11. Shannon RD. *Acta Crystallogr., Sect. A* 1976; **32**: 751–767.
12. Woodruff WH, Pastor RW, Dabrowiak JC. *J. Am. Chem. Soc.* 1976; **98**: 7999–8006.
13. Szymanski HA. *Infrared Band Handbook.* Plenum Press: New York, 1963; 106–113.
14. Trommsdorff HP, Sahy P, Kahane-Paillous J. *Spectrochim. Acta, Part A* 1970; **26**: 1135–1147.
15. Girlando A, Zanon I, Bozio R, Pecile C. *J. Chem. Phys.* 1978; **68**: 22–31.
16. Girlando A, Pecile C. *Spectrochim. Acta, Part A* 1973; **29**: 1859–1878.
17. Dixon DA, Miller JS. *J. Am. Chem. Soc.* 1987; **109**: 3656–3664.